

## Coulomb Blockade and Hopping Conduction in PbSe Quantum Dots

Hugo E. Romero and Marija Drndić\*

*Department of Physics and Astronomy, University of Pennsylvania, Philadelphia, Pennsylvania 19104, USA*

(Received 31 January 2005; published 3 October 2005)

We report for the first time on rich and tunable transport phenomena in closed-packed arrays of PbSe colloidal nanocrystals (NCs) in the form of thin films. As the interdot coupling is increased, the system evolves from an insulating regime dominated by Coulomb blockade to a semiconducting regime, where hopping conduction is the dominant transport mechanism. The observed phenomena can be interpreted using the framework established mainly in the context of transport measurements in metallic quantum dots and disordered semiconductors.

DOI: [10.1103/PhysRevLett.95.156801](https://doi.org/10.1103/PhysRevLett.95.156801)

PACS numbers: 73.63.Kv, 05.60.Gg, 73.21.Cd, 73.22.-f

Closed-packed arrays of nanocrystals, or quantum dots (QDs), form a new class of “artificial solids” with tunable properties that are controlled at the nanoscale [1]. QD solids offer opportunities to realize model systems to test the Hubbard model and investigate the cooperative physical phenomena that develop when the interdot coupling (the tunnel matrix element) between neighboring particles and the degree of long-range Coulomb interactions are tuned. QD solids also provide media for potential novel electronic, optical, and optoelectronic applications that combine the unique properties of individual QDs and the collective properties of coupled QDs.

Even though these systems consist of metallic and semiconducting building blocks, the collective properties of nanocrystal (NC) arrays have proven to be complex and not easily predictable from a theoretical standpoint, which would require solving a Hubbard model. Thus, even the simplest NC array—a closed-packed single layer of metal NCs—remains poorly understood. However, with NC arrays as artificial solids expected to provide useful analogs and tunable test beds for various bulk correlated electron systems, a full understanding of NC monolayers is vital.

Colloidal PbSe NCs offer unique access to the regime of extreme quantum confinement and are expected to have significantly different physical properties from those of better-known II-VI NCs [2]. Because of the large dielectric constant of PbSe ( $\epsilon_m = 23$ ), better charge screening is expected, leading to more conductive arrays. Here, we report on the rich transport phenomena observed in PbSe NCs arrays. Specifically, undoped PbSe-NC arrays exhibit high-temperature  $T$  ( $T > 300$  K) Coulomb blockade phenomena, activated hopping, and direct quantum tunneling, depending on the interdot coupling and  $T$ . In addition, conductivity can be varied over more than 10 orders of magnitude.

The emergence of such a variety of transport regimes in PbSe-NC arrays has been elusive for other semiconductor and metallic NC arrays, where only either variable-range-hopping conduction [3] or Coulomb blockade transport [4] has been observed. Our observations imply that PbSe-NC

arrays are more robust and forgiving than those systems that might be strongly affected by the local environment. This, in turn, has important practical and fundamental consequences.

PbSe NCs used in this study had a mean diameter of  $\sim 5.5$  nm with  $< 5\%$  size distribution [5]. They were capped with oleic acid, which provided a 1 nm-thick insulating coat. NCs were not subjected to any chemical treatment and were exposed to ambient air only briefly ( $< 5$  min) while loading the cryostat. PbSe-NC superlattices, one to three monolayers thick, were prepared by drop casting a 9:1 hexane/octane solution onto lithographically prepatterned Si substrates covered with a 300 nm layer of SiO<sub>2</sub>. The doped Si substrate was used as a grounded back gate. The patterns are arrays of paired 800  $\mu\text{m}$ -wide Ti/Au electrodes with a gap of 1.5–2  $\mu\text{m}$ , resulting in  $N \times M$  arrays of  $N = 200$ –360 particles in length and  $M \sim 10^5$  particles wide. Prior to film deposition, the Si substrates were treated for 10 min under O<sub>2</sub> plasma to reduce organic surface contamination. This procedure resulted in long-range-order hcp assembly of NCs with domain size comparable to the electrode’s spacing [6]. The isolation between the contact pads before film deposition was measured to be  $> 10$  P $\Omega$  at 600 K, and even higher at lower  $T$ . Electrical transport measurements were carried out as a function of  $T$  from 77 to 600 K in a liquid N<sub>2</sub> cryostat under a dynamic vacuum of  $< 10^{-6}$  Torr. A bias voltage  $V_{\text{bias}}$  was applied to the drain electrode and the current  $I$  at the source was monitored with a virtual-earth current amplifier.

As-deposited PbSe films are very resistive and negligible current ( $< 10$  fA) flows up to  $V_{\text{bias}} = \pm 200$  V, which corresponds to a resistance  $R > 20$  P $\Omega$  at 300 K. These samples are initially uncharged and charges diffuse slowly into the system once  $V_{\text{bias}}$  is turned on [7]. The high dark electrical  $R$  of as-deposited thin films is due to high potential barriers between NCs. *In situ* heating in vacuum significantly decreased  $R$  [8]. This phenomenon of increasing conductivity upon vacuum annealing is due to heat-induced reduction of the interdot separation [9].

Negligible conduction between the electrodes was observed upon deposition and heating of oleic acid alone. Transmission electron microscopy (TEM) images show that the separation  $s$  between NCs decreases with annealing (cf. Figures 2(a) and 2(b), upper inset); eventually NCs will get in close contact when the oleic acid coat is completely removed. We studied electrical transport on samples vacuum annealed only up to 523 K, to minimize ligand decomposition/desorption [10] and NC melting or sintering [11]. Here, we present the results from a sample annealed at and *measured* up to incremental  $T$  of 373, 473, and 523 K [12]. The reported behavior is typical of the six devices that we have measured.

**Coulomb blockade regime.**—Figure 1 shows  $I$ - $V_{\text{bias}}$  curves as a function of  $T$  for a PbSe sample vacuum-annealed at 373 K. All of the curves are nonlinear, slightly asymmetric and hysteretic. Further studies are underway to determine the origin of the hysteretic-type behavior observed in the  $I$ - $V_{\text{bias}}$  curves. We should mention, however, that the measured  $I$  is entirely independent of history and sweep rate for forward sweeps.  $I$ - $V_{\text{bias}}$  curves in Fig. 1 also exhibit a clear threshold voltage  $V_{\text{th}}$ , characteristic of Coulomb blockade of transport. Below  $V_{\text{th}}$ ,  $I \sim 0$ . A conduction gap is usually observed when the overall charging energy of a QD satisfies  $E_C \gg k_B T$ . In our case,  $E_C \sim 36$  meV [13] and a Coulomb gap is expected only at  $T \ll 410$  K.

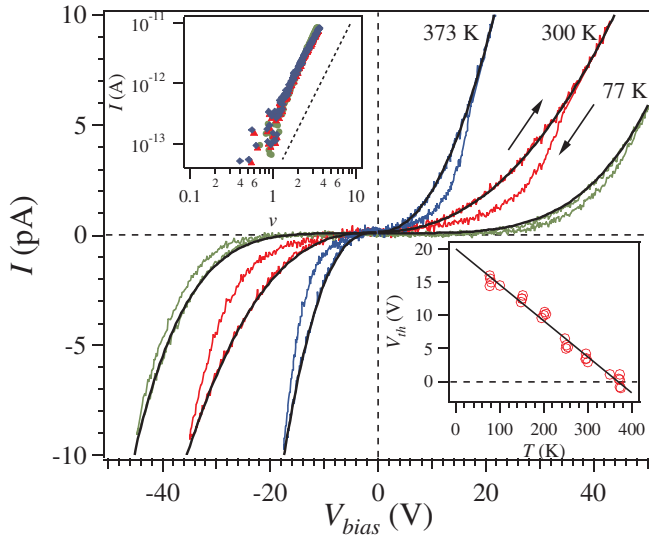


FIG. 1 (color online).  $I$ - $V_{\text{bias}}$  characteristics at three representative  $T$  for a PbSe-NC array vacuum annealed *in situ* at 373 K. The arrows show the direction of sweeping  $V_{\text{bias}}$  at a rate of 100 mV/s. The solid lines are fits to the data using Eq. (1). The upper inset shows the scaling behavior of  $I$  with normalized excess voltage  $v = V/V_{\text{th}} - 1$ , where the dotted line corresponds to  $\zeta = 2.4$ . The lower inset shows the  $T$  dependence of  $V_{\text{th}}$  for all samples measured. Here, the solid line is a linear fit to the data.

Interestingly, many of the properties of the sample represented in Fig. 1 could be understood in the framework of the model of collective charge transport in arrays of normal-metal QDs, proposed by Middleton and Wingreen (MW) [14]. The current (for  $V > V_{\text{th}}$ ) through a small uniform array of metallic QDs separated by tunnel barriers follows the relation

$$I = I_0(V - V_{\text{th}})^\zeta, \quad (1)$$

where the scaling exponent  $\zeta = 1$  and  $5/3$  in the 1D and 2D case, respectively, [14]. Solid lines in Fig. 1 are fits of the data to Eq. (1) with  $T$ -independent exponent  $\zeta = 2.4 \pm 0.1$ . In our NC devices, we found that the size-dependent exponent is  $2.1 < \zeta < 2.6$  ( $\Delta\zeta/\zeta \sim 6\%$ ). This is in good agreement with previous observations and simulations of 2D and 3D transport, where  $\zeta$  ranges from  $\sim 2$  to 3.5, depending on film thickness [14,15].

We found relatively high  $V_{\text{th}}$  values. For instance,  $V_{\text{th}} \sim 3$  V at 300 K and increases to  $\sim 14.4$  V at 77 K. All our devices show a distinct  $V_{\text{th}}$ , although the specific value of  $V_{\text{th}}$  at a given  $T$  varies (e.g.,  $V_{\text{th}} = 3.5 \pm 0.5$  V at 300 K) from device to device due to offset-charge disorder in the array [14]. Large values of the measured  $V_{\text{th}}$  are due to a collective effect. If the effect were due to a single particle in the array, then  $V_{\text{th}} = e/2C_g \sim 125$  meV. The MW model, however, predicts that  $V_{\text{th}}$  is directly proportional to the size of the array  $N$ .

Furthermore, we observed parallel shift of the  $I$ - $V_{\text{bias}}$  curves along the  $V_{\text{bias}}$  axis with  $T$ , i.e., the  $I$ - $V_{\text{bias}}$  curves keep their nonlinear, low- $T$  shape and simply shift to lower  $V_{\text{bias}}$  with increasing  $T$ . The estimated  $V_{\text{th}}$  values thus produced a scaling behavior of the  $I$ - $V_{\text{bias}}$  curves (Fig. 1, upper inset).

Another interesting aspect of the  $I$ - $V_{\text{bias}}$  curves is that, above  $T^* \sim 360$  K,  $V_{\text{th}}$  first vanishes and then becomes negative (Fig. 1, lower inset). This phenomenon was first observed in Coulomb blockade studies in Au nanocluster films and interpreted as due to transport over a barrier [16,17]. At  $T \geq T^*$ , the sample also exhibits nonzero zero-bias conductance  $G$  that increases with  $T$ .

For all arrays studied,  $V_{\text{th}}$  decreases linearly with increasing  $T$  up to  $T = 373$  K and we would expect  $V_{\text{th}} \sim 20$  V at 0 K for our six samples (Fig. 1, lower inset). A similar trend was also noticed in 1D chains of carbon nanospheres [18], single-layer Au nanocluster films [16], and monolayers of Au NCs [17]. Parthasarathy *et al.* [17] developed a model in which thermal fluctuations provide the energy to overcome the local threshold in a fraction of the junctions to shift the global threshold of the array in the form  $V_{\text{th}}(T) = V_{\text{th}}(0)[1 - 4.8k_B T P(0)/p_c]$ , where  $1/P(0)$  is an effective charging energy that depends on  $r$  and the interdot distance, and  $p_c$  is the percolation threshold of the underlying lattice. For a 2D hcp lattice  $p_c \sim 0.347$  [17]. These predictions agree well with our data (Fig. 1, lower inset). We determined  $1/P(0) \sim 0.44$  eV from data fitting.

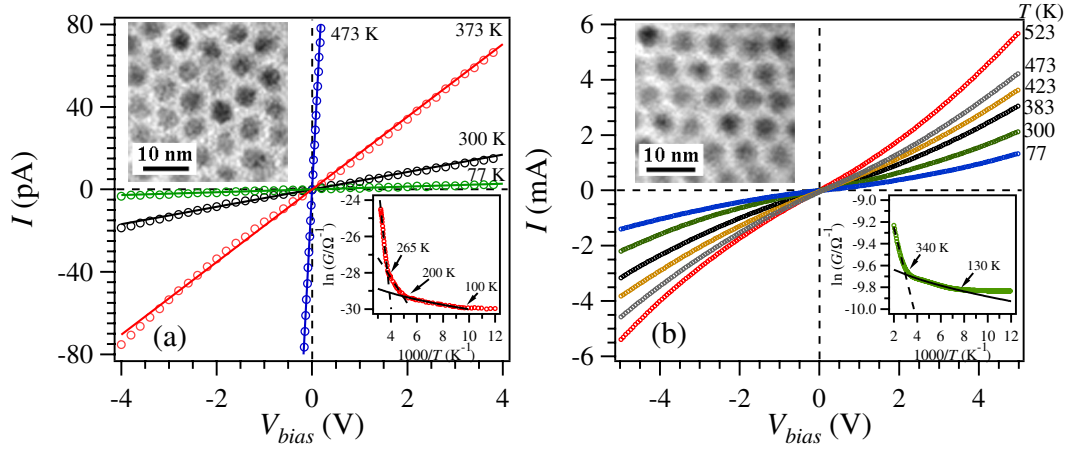


FIG. 2 (color online).  $I$ - $V_{\text{bias}}$  characteristics versus  $T$  for a PbSe-NC array vacuum annealed *in situ* at (a) 473 and (b) 523 K.  $V_{\text{bias}}$  was swept at 100 mV/s. The solid lines in (a) are linear fits to the data. The lower insets show  $G$  (in log scale) versus the inverse of  $T$ . Here, the solid and dashed lines are fits of Eq. (2) to the data, using  $p = 1/2$  and 1, respectively. The upper insets are TEM images of PbSe-NC arrays on thin amorphous carbon films, after vacuum annealing at 0.5 K/min.

Using the estimated  $N \approx 220$ , we obtained  $1/P(0) = eV_{\text{th}}(0)/\alpha N \sim 0.40$  eV, in good agreement with our experiment [19]. In general, PbSe-NC arrays annealed up to 373 K behave as “high- $T$ ” ( $T > 300$  K) Coulomb blockade devices.

**Hopping conduction regime.**—Figure 2(a) shows  $I$ - $V_{\text{bias}}$  curves as a function of  $T$  for a PbSe sample vacuum annealed at 473 K. All of the curves appear Ohmic and  $R$  decreases monotonically with  $T$ . They are highly symmetric and nonhysteretic. None of the  $I$ - $V_{\text{bias}}$  curves shows Coulomb blockade behavior.

The dependence of  $\ln G$  with the inverse of absolute  $T$  for this sample is shown in the lower inset to Fig. 2(a). Several distinct regions are clearly observed, similar to disordered semiconductors [20].  $\ln G(T)$  showed a linear dependence above 265 K and in the  $T$  range  $200 \text{ K} < T < 265 \text{ K}$ . Below 200 K, a quasilinear region is observed and the  $T$  dependence is much weaker than at high  $T$ .

For a disordered system,  $G(T)$  may be expressed as

$$G(T) = G_0 \exp[-(T_0/T)^p], \quad (2)$$

where the preexponential factor  $G_0$  may be independent of  $T$  or a slowly varying function of  $T$ , while  $T_0$  is a constant of the material. The value of  $p$ , ranging from  $1/4$  to 1, depends on the  $T$  range of measurement and the nature of the transport process operative in the sample. In order to determine the value of  $p$  in our samples, we studied  $G(T)$  in all  $T$  regions by fitting Eq. (2) to our data, using a least-square fitting procedure. For all samples, it was observed that  $p \sim 0.95$ – $1.05$  in the high- $T$  regions and decreases to  $\sim 0.48$ – $0.55$  in the low- $T$  regions. Best fit values of  $T_0$  were obtained by fixing  $p$  to the average value of either 1 or  $1/2$ .

The observed Arrhenius-like  $T$  dependence at high  $T$  ( $T > 265$  K) is typical of a simple, thermally activated process. Here,  $G = G_0 \exp(-E_a/k_B T)$ , where  $E_a$  is the activation energy for charge transport. From the slope of

the Arrhenius plot we found  $E_a \sim 0.6$  eV. In all our PbSe-NC samples, we calculated  $E_a = 0.5 \pm 0.1$  eV. Generally, for an *intrinsic* semiconductor,  $E_a = E_g/2$ . In intrinsic semiconductor NCs, charge carriers at conduction or valence orbitals must also overcome the Coulomb barrier  $\Delta E$  before they can take part in conduction. Thus,  $E_a = E_g/2 + \Delta E$ . We associate  $\Delta E$  with the maximum charging energy of the QD array with weak capacitive coupling between neighbors. Assuming  $\Delta E = 0.1$  eV  $\sim 3E_C$  then  $E_g \sim 1$  eV, in reasonable agreement with  $E_g \sim 0.8$  eV, as determined from optical absorption measurements. Our PbSe-NC arrays may then possess an intrinsic electrical conductivity due to thermal activation of carriers across  $E_g$  with the subsequent carriers hopping between nearest neighbors (NNH).

In the  $T$  range  $200 \text{ K} < T < 265 \text{ K}$ , Arrhenius-like  $T$  dependence is also observed. A smaller  $E_a \sim 95$  meV dominates the transport in this  $T$  region. We note that  $E_a \sim \Delta E$ , so the density of thermally excited QDs is negligible in this  $T$  region and electrical conduction may result from NNH.

In the low- $T$  region ( $T < 200$  K),  $G(T)$  is best described by the expression,  $G = G_0 \exp[-(T_0/T)^{1/2}]$ . This is the typical  $T$  dependence of the Efros-Shklovskii variable-range hopping (ES-VRH), where  $T_0 \approx 2.8e^2/4\pi\epsilon_0\epsilon_m\xi k_B$  and  $\xi$  is the localization length or the decay length of the electronic wave function [21]. In this picture, charge carriers have a higher probability of hopping across distant sites. Using  $T_0 \sim 600$  K from the data fitting, we estimated  $\xi \sim 3.5$  nm, which is consistent with  $r$ . ES-VRH was recently reported on *n*-type CdSe NC films as well [3]. The fact that transport in semiconductor NC arrays could result from ES-VRH is intriguing and difficult to explain because neutral QDs have a hard charging gap at the Fermi level. The characteristic  $T^{-1/2}$  dependence of

$G(T)$  is also a distinct signature of grain size nonuniformity in some disordered materials [22]. In this case, conduction is due to NNH from thermally charged QDs to neutral QDs.

To gain additional insight into the nature of the hopping conduction mechanism in PbSe-NC arrays, we further tuned the interdot coupling by a vacuum-annealing procedure. Figure 2(b) shows the  $I-V_{\text{bias}}$  characteristics as a function of  $T$  for the device heated at 523 K. All of the curves are symmetric and show no hysteresis. The  $I-V_{\text{bias}}$  curves have a sigmoid shape, with a change of slope at low bias ( $\pm 0.1\text{--}0.2$  V). The sample is highly conductive. Even without any doping, this sample is  $\sim 3$  orders of magnitude more conductive than the  $n$ -doped and annealed CdSe QDs arrays recently reported [3].

The lower inset to Fig. 2(b) shows the variation of  $\ln G$  with the inverse of absolute  $T$  for this device.  $\ln G(T)$  reached a plateau below 130 K—an indication of direct, interdot quantum tunneling as the conduction mechanism. In the intermediate  $T$  range ( $130\text{ K} < T < 340\text{ K}$ ),  $\ln G(T)$  follows a  $T^{-1/2}$  dependence. Assuming ES-VRH, we estimated  $T_0 \sim 20$  K and  $\xi \sim 102$  nm. The large value of  $\xi$  indicates the reduction of the barrier heights between the NCs and indicates that charge carriers can hop between distant sites. Above  $T_a = 340$  K, Arrhenius-like  $T$  dependence is observed and  $E_a \sim 38$  meV, in agreement with  $E_C$ . This simple type of activated conduction arises when the mean hopping distance approaches the value of the distance between neighboring islands  $D$ , so the conduction process would correspond to NNH. Using  $T_a = (\xi/4D)^2 T_0$ , we determined  $D \sim 6.2$  nm, which corresponds to  $s = 0.7$  nm. Although ES-VRH could explain our results, microscopic models for NC arrays are needed to fully understand the mechanism leading to a  $T^{-1/2}$  dependence of  $\ln G(T)$ .

In conclusion, this work demonstrates the rich and variable transport behavior in undoped, semiconductor QD artificial solids studied in a wide  $T$  range ( $77\text{ K} \leq T \leq 523\text{ K}$ ). The observed effects are robust and preset by the highest  $T$  at which the samples were measured. Conduction can be varied from the insulating to the semiconducting limit by controlling the strength of the interdot coupling, with a concomitant increase in the conductivity. These results could have important implications for the proposed applications of PbSe NCs, such as optoelectronic devices.

We acknowledge help from G. Calusine with TEM imaging and helpful discussions with D. S. Novikov. This work was supported in part by the ONR Young Investigator Grant No. N000140410489, the ACS PRF Grant No. 41256-G10, and NSF Grant No. DMR-0449553.

\*To whom correspondence should be addressed.  
Electronic address: drndic@physics.upenn.edu

- [1] C. P. Collier, T. Vossmeier, and J. R. Heath, *Annu. Rev. Phys. Chem.* **49**, 371 (1998).
- [2] F. W. Wise, *Acc. Chem. Res.* **33**, 773 (2000).
- [3] D. Yu, C. J. Wang, B. L. Wehrenberg, and P. Guyot-Sionnest, *Phys. Rev. Lett.* **92**, 216802 (2004).
- [4] R. Parthasarathy, X.-M. Lin, and H. M. Jaeger, *Phys. Rev. Lett.* **87**, 186807 (2001).
- [5] PbSe NCs, dispersed in hexane, were obtained from Evident Technologies, Inc.
- [6] Same amounts of the same NC solutions used in our studies, deposited on TEM carbon-coated grids, yielded one to two monolayers of NCs with long-range hcp order of several 100's of nm.
- [7] Z. Hu, M. D. Fischbein, and M. Drndic, *Nano Lett.* **5**, 1463 (2005).
- [8] For instance, a heat treatment at  $150^\circ\text{C}$  resulted in an asymptotic  $R \sim 200$  k $\Omega$  (i.e., more than 10 orders of magnitude lower than for an untreated device). Vacuum annealing at  $300^\circ\text{C}$  asymptotically reduced  $R$  by more than 14 orders of magnitude—down to 250  $\Omega$ .
- [9] M. Drndic, M. V. Jarosz, N. Y. Morgan, M. A. Kastner, and M. G. Bawendi, *J. Appl. Phys.* **92**, 7498 (2002).
- [10] Thermogravimetric curves show that oleic acid removal takes place in two distinct steps: a small weight loss at  $120^\circ\text{C}$  due to desorption of weakly bound oleic acid, and a large weight loss at  $280^\circ\text{C}$  as a result of complete removal of oleic acid from the NC surface.
- [11] F. Chen, K. L. Stokes, W. Zhou, J. Fang, and C. B. Murray, *Mater. Res. Soc. Symp. Proc.* **691**, 359 (2002).
- [12] Similar results are obtained when samples are annealed directly to the final  $T$ .
- [13]  $E_C = e^2/(C_g + 9C)$ , where  $C_g$  and  $C$  are, respectively, the self-capacitance (or capacitance to the gate) and mutual capacitance of QDs. The factor of 9 is the average number of nearest neighbors of each NC in a superlattice of one to three monolayers thick. In our case,  $C_g \approx 4\pi\epsilon_0\epsilon r \sim 0.6$  aF and  $C \approx 2\pi\epsilon_0\epsilon r \ln[(2r+s)/s] \sim 0.4$  aF, where  $r = 2.75$  nm is the NC radius,  $\epsilon = 2.1$  the dielectric constant of the tunnel barriers due to oleic acid surfactant, and  $s = 2$  nm the spacing between NCs.
- [14] A. A. Middleton and N. S. Wingreen, *Phys. Rev. Lett.* **71**, 3198 (1993).
- [15] A. S. Cordan, Y. Leroy, A. Goltzene, A. Pepin, C. Vieu, M. Mejias, and H. Launois, *J. Appl. Phys.* **87**, 345 (2000).
- [16] M. G. Ancona, W. Kruppa, R. W. Rendell, A. W. Snow, D. Park, and J. B. Boos, *Phys. Rev. B* **64**, 33408 (2001).
- [17] R. Parthasarathy, X.-M. Lin, K. Elteto, T. F. Rosenbaum, and H. M. Jaeger, *Phys. Rev. Lett.* **92**, 076801 (2004).
- [18] A. Bezryadin, R. M. Westervelt, and M. Tinkham, *Appl. Phys. Lett.* **74**, 2699 (1999).
- [19]  $\alpha N$  is the number of up steps in the optimal path (minimum number of up steps) across the array at  $T = 0$ . For a hcp lattice of spheres  $\alpha = 0.227$  [17].
- [20] N. F. Mott and E. A. Davis, *Electronic Processes in Non-Crystalline Materials* (Clarendon, New York, 1979).
- [21] B. I. Shklovskii and A. L. Efros, *Electronic Properties of Doped Semiconductors* (Springer-Verlag, Berlin, 1984).
- [22] B. Abeles, P. Sheng, M. D. Coutts, and Y. Arie, *Adv. Phys.* **24**, 407 (1975).